

Palmitic acid inhibits vascular smooth muscle cell switch to synthetic phenotype via upregulation of miR-22 expression

Yanchao Hu¹, Yajie Fan¹, Chunyan Zhang¹, Congxia Wang^{1,&}

¹Department of Cardiovascular Medicine, The Second Affiliated Hospital of Xi'an Jiaotong University, Shaanxi, Xi'an 710004, China

Correspondence to: Congxia Wang; email: wxcirculation@163.com, <https://orcid.org/0000-0002-3423-4644>

Keywords: VSMC, palmitic acid, synthetic phenotype, miR-22

Received: August 17, 2022

Accepted: October 3, 2022

Published: October 12, 2022

Copyright: © 2022 Hu et al. This is an open access article distributed under the terms of the [Creative Commons Attribution License](https://creativecommons.org/licenses/by/3.0/) (CC BY 3.0), which permits unrestricted use, distribution, and reproduction in any medium, provided the original author and source are credited.

ABSTRACT

Synthetic phenotype switch of vascular smooth muscle cells (VSMCs) has been shown to play key roles in vascular diseases. Mounting evidence has shown that fatty acid metabolism is highly associated with vascular diseases. However, how fatty acids regulate VSMC phenotype is poorly understood. Hence, the effects of palmitic acid (PA) on VSMC phenotype were determined in this study. The effect of the PA on VSMCs was measured by live/dead and EdU assays, as well as flow cytometry. Migration ability of VSMCs was evaluated using transwell assay. The underlying targets of miR-22 were predicted using bioinformatics online tools, and confirmed by luciferase reporter assay. The RNA and protein expression of certain gene was detected by qRT-PCR or western blot. PA inhibited VSMC switch to synthetic phenotype, as manifested by inhibiting VSMC proliferation, migration, and synthesis. PA upregulated miR-22 in VSMCs, and miR-22 mimics exerted similar effects as PA treatment, inhibiting VSMC switch to synthetic phenotype. Inhibition of miR-22 using miR-22 inhibitor blocked the impacts of PA on VSMC phenotype modulation, suggesting that PA modulated VSMC phenotype through upregulation of miR-22 expression. We found that ecotropic virus integration site 1 protein homolog (EVI1) was the target of miR-22 in regulation of VSMC phenotype. Overexpression of miR-22 or/and PA treatment attenuated the inhibition of EVI1 on switch of VSMCs. These findings suggested that PA inhibits VSMC switch to synthetic phenotype through upregulation of miR-22 thereby inhibiting EVI1, and correcting the dysregulation of miR-22/EVI1 or PA metabolism is a potential treatment to vascular diseases.

INTRODUCTION

Vascular function is largely dependent on vascular smooth muscle cells (VSMCs). Different from the skeletal muscle cells or cardiomyocytes, VSMCs remain possessing remarkable phenotypic plasticity in response to multiple stimuli [1]. VSMCs switch from a contractile state to a dedifferentiated, synthetic phenotype, playing crucial roles in several vascular diseases [2–4]. The synthetic phenotype induces migration to the intima and enhances proliferation and extracellular matrix protein synthesis, thereby resulting in an impaired contractility of VSMC [5]. Therefore, exploration of the underlying mechanisms involved in

VSMC phenotypic switch regulation is important in vascular diseases.

There are multiple environmental stimuli have been identified as factors which lead to VSMC phenotype switch, such as growth factors, reactive oxidative species (ROS), and mechanical injury [6, 7]. Recent studies have shown that metabolites were also involved in regulation of VSMC phenotype [8]. For example, lactate, a product of glucose metabolism, was found to promote the synthetic phenotype of VSMCs, which links glucose metabolism to VSMC phenotypic switch [8]. Mounting evidence has shown that fatty acid metabolism is abnormal in vascular diseases, which

plays an important role in the development of atherosclerosis and other vascular diseases [9, 10]. These advances suggest that fatty acids metabolism may play a role in regulation of VSMC phenotype. However, how fatty acids regulate VSMC phenotype is poorly understood. As the most common saturated fatty acid found in organism, palmitic acid (PA) serves as an energy source or component of partially biochemicals and cellular structures. The circulating level of PA is increased in metabolic disorders and correlated with the adverse outcomes of cardiovascular diseases [11–13]. Here, we aimed to examine the impacts and underlying mechanism of PA on VSMC phenotype.

VSMC phenotype switch has been widely studied in transcriptional and epigenetic levels [14, 15]. We were very interested in the growing evidence supporting a critical role for miRNAs in regulating VSMC differentiation and phenotypic switch [16, 17]. A series of miRNAs have been reported as regulators of VSMC phenotype, including miR-21 [18], miR-22 [16], miR-23b [19], miR-100 [20], miR-124 [16], miR-133 [21], miR-143/145 [22], miR-146a [23], miR-195 [24], miR-221/222 [25] and miR-424 [26]. Here, we found that PA inhibits VSMC switch to synthetic phenotype via upregulation of miR-22. These results suggested that PA plays a role in regulation of VSMC phenotype.

METHODS

Cell culture

Primary VSMCs were isolated from 8–10 weeks old male SD rat (weighed 170–250 g) thoracic aorta as reported previously [27]. Briefly, thoracic aortas were excised followed by phosphate buffered saline (PBS) washing for 3 times. After these, the aortic media layer was dissected, cut into pieces, and seeded onto a 6-well plate. Cells were maintained in DMEM supplemented with 10% fetal bovine serum (FBS), 1% penicillin and streptomycin at 37°C in a humidified incubator with 5% CO₂ in atmosphere for 2 weeks. All animal procedures in this study were conducted in accordance with the National Institutes of Health Guidelines on the Use of Laboratory Animals, and were approved by the Xi'an Jiaotong University Second Affiliated Hospital.

Live/dead cell assay

The 2-color fluorescence with the LIVE/DEAD Viability/Cytotoxicity kit (Molecular Probes) was used to quantify the living and dead cells in this study as directed by the manufacturer's protocol. Briefly, cells were harvested after treatment, washed with PBS twice, and incubated with 300 µl of live/dead solution for half an hour at 37°C in the dark room. Then, the

fluorescence was read using a microplate reader (FLUOstar® Omega).

EdU assay

Proliferation of VSMCs was analyzed using the Click-it EdU kit (C10086, Invitrogen, USA). Briefly, cells were seeded on the slides at a density of 1.0×10^3 cells in 12-well plate each well. After treatment, cells were incubated with 50 µmol/L EdU solution at 37°C for 2 h. Then, cells were washed with cooled PBS for twice and fix 4% PFA at 4°C for 15 min. Following this, 100 µl Apollo reaction cocktail was added into cells followed by nucleus staining with Hoechst 33342 according to the manufacturer's protocol. The fluorescence signal was then analyzed under a fluorescence microscope. EdU incorporation (%) = EdU positive cells/(EdU-positive cells + Hoechst-positive cells) × 100%.

Apoptosis determination

The apoptosis of VSMCs was detected using an Annexin V-FITC apoptosis detection kit (C1062, Beyotime, China). Briefly, cells were collected after treatment, washed with cooled PBS twice, resuspended with 1 mL AnnexinV-FITC, and maintained for 10 min at room temperature according to the kit's protocol. Following this, cells were subjected to flow cytometry analysis.

Transwell assay

VSMCs were seeded in the upper chamber of transwell (12 µm) and placed in a 24-well plate at a density of 1.0×10^5 cells/well in 200 µl DMEM contained with 0.5% FBS. The lower chamber was filled up with 600 µl DMEM contained with 10% FBS. After incubation with for 24 h, medium was discarded and the lower chamber membrane was fixed with methanol at room temperature for 15 min. Subsequently, cells were stained with 0.1 crystal violet-methanol solution for 15 min at room temperature. Finally, the migrated cells were pictured and calculated under a light microscope.

Real-time reverse transcription PCR

RNAiso Plus reagent (Code No.: 9108, Takara) was used for the RNA isolation as the manufacturer recommended. The cDNA was synthesized using the isolated RNA (500 ng/sample) and amplification of certain genes was performed using a SYBR Green PCR kit (Takara) in a CFX200 (Bio-Rad) with the cycles of 95°C for 10 min and 40 cycles of 95°C for 5 s, 58°C for 30 s, and 72°C for 10 s. The mRNA level of each

gene was normalized to housekeeping gene, namely, GAPDH or U6. The primer sequences are listed in Supplementary Table 1.

Cell transfection

MiR-22 mimics (5'-AAGCUGCCAGUUGAAGAA CUGU-3'), miR-23b mimics (5'-AUCACAUUGCCA GGGAUUACCAC-3'), miR-125b mimics (5'-UCCUGAGACCCUAACUUGUGA-3'), negative control mimics (NC mimics, #miR1N0000001-1-10), miR-22 inhibitors (5'-ACAGUUCUCAA CUGGCAGCUU-3'), and NC inhibitors (#miR2N0000001-1-10) were synthesized by RIBOBIO Co., Ltd Chin (Guangzhou, China). Empty vector (pcDNA3.1) and EVI1 overexpression plasmid (pcDNA3.1-EVI1 OE) were purchased from GeneChem (Shanghai, China). miRNA mimics (100 nmol/L), inhibitors (200 nmol/L), or NC (5'-UUCUCCGAACGUGUCACGUTT-3') (100 nmol/L) were transfected using Lipofectamine™ 3000 (Invitrogen) according to manufacturer's instruction. After 60 h post-transfection, the transfected cells were harvested and utilized for further analyses.

Dual-luciferase reporter assay

Wt and Mt ecotropic virus integration site 1 protein homolog (*EVI1*) 3'UTR sequence was acquired using PCR method, and then cloned into SpeI and HindIII sites of pMir-Report Luciferase vector (Applied Biosystems). The resulting construct was transfected (5ng) into 293T cells with 20 nM control mimics or miR-22 mimics using Lipofectamine-2000 (Invitrogen). After 24 h post-transfection, luciferase activity of cells was assessed using a Luciferase Assay System (Promega).

Western blot

For immunoblotting, proteins were isolated from cells using RIPA buffer. Total protein extracts (15–50 µg) were separated using sodium dodecyl sulfate polyacrylamide gel electrophoresis and transferred onto polyvinylidene fluoride membrane. Membranes were then probed with anti-bax (1:2000; #ab32503; Abcam), bcl-2 (1:2000; #ab196495; Abcam), cleaved-caspase-3/caspase-3 (1:2000; #ab184787; Abcam), SM22α (1:2000; #ab14106; Abcam), calponin (1:500; #ab227661; Abcam), SMMHC (1:2000; #ab125884; Abcam), vimentin (1:2000; #ab92547; Abcam), collagen I (1:1000; #ab270993; Abcam), osteopontin (OPN; 1:1000; #ab63856; Abcam), LAMC1 (1:1000; #ab233389; Abcam), EVI1 (1:1000; #SAB2100723; Sigma), AKT3 (1:2000; #ab152157; Abcam), TP53INP1 (1:2000; #ab202026; Abcam), and β-actin (1:2000; #ab8226; Abcam) at room temperature for

1.5 h. Then, membranes were immersed with the HRP-conjugated secondary antibody at room temperature for 1 h. Following this, the BM chemiluminescence blotting system (Thermo Scientific) was used for detection and protein bands were quantified using Image J software (NIH, USA).

Statistical analysis

All data are presented as mean ± standard deviation, and comparisons were performed using one-way ANOVA or two-way ANOVA followed by an unpaired *t*-test, as appropriate. *P* < 0.05 was considered statistically significant.

Availability of data and materials

The datasets used and/or analyzed during the present study are available from the corresponding author upon reasonable request.

RESULTS

PA inhibited the synthetic phenotype in cultured VSMCs

VSMCs were treated with PA (0, 100, 200 or 400 µM) for 3 d. Live/Dead assay suggested that PA treatment decreased cell viability, and increased cell death in a dose-dependent manner in VSMCs (Figure 1A). Moreover, EdU assay suggested that PA treatment significantly decreased the EdU incorporation of VSMCs in a dose-dependent manner (Figure 1B and 1C). Further analysis indicated that PA treatment could significantly increase VSMCs apoptosis (Figure 1D and 1E). Western blot analysis presented that PA treatment markedly increase the Bax and cleaved-caspase-3 expression but decreased Bcl-2 expression (Figure 1F). These findings suggested that PA may inhibit the VSMC switch to synthetic phenotype. In addition, PA treatment (200 µM) suppressed the migration of VSMCs as detected by transwell assay (Figure 1G). Furthermore, PA treatment (200 µM) for 3 d increased protein levels for markers of the contractile phenotype, including α-SMA, calponin, and SMMHC, and decreased protein levels of the synthetic phenotype, including vimentin, collagen I, and osteopontin (OPN) (Figure 1H). These results reinforced the notion that PA inhibits the VSMC switch to synthetic phenotype.

PA increased miR-22 expression in VSMCs

To test whether miRNA is involved in regulation of VSMC phenotype switch induced by PA, the report

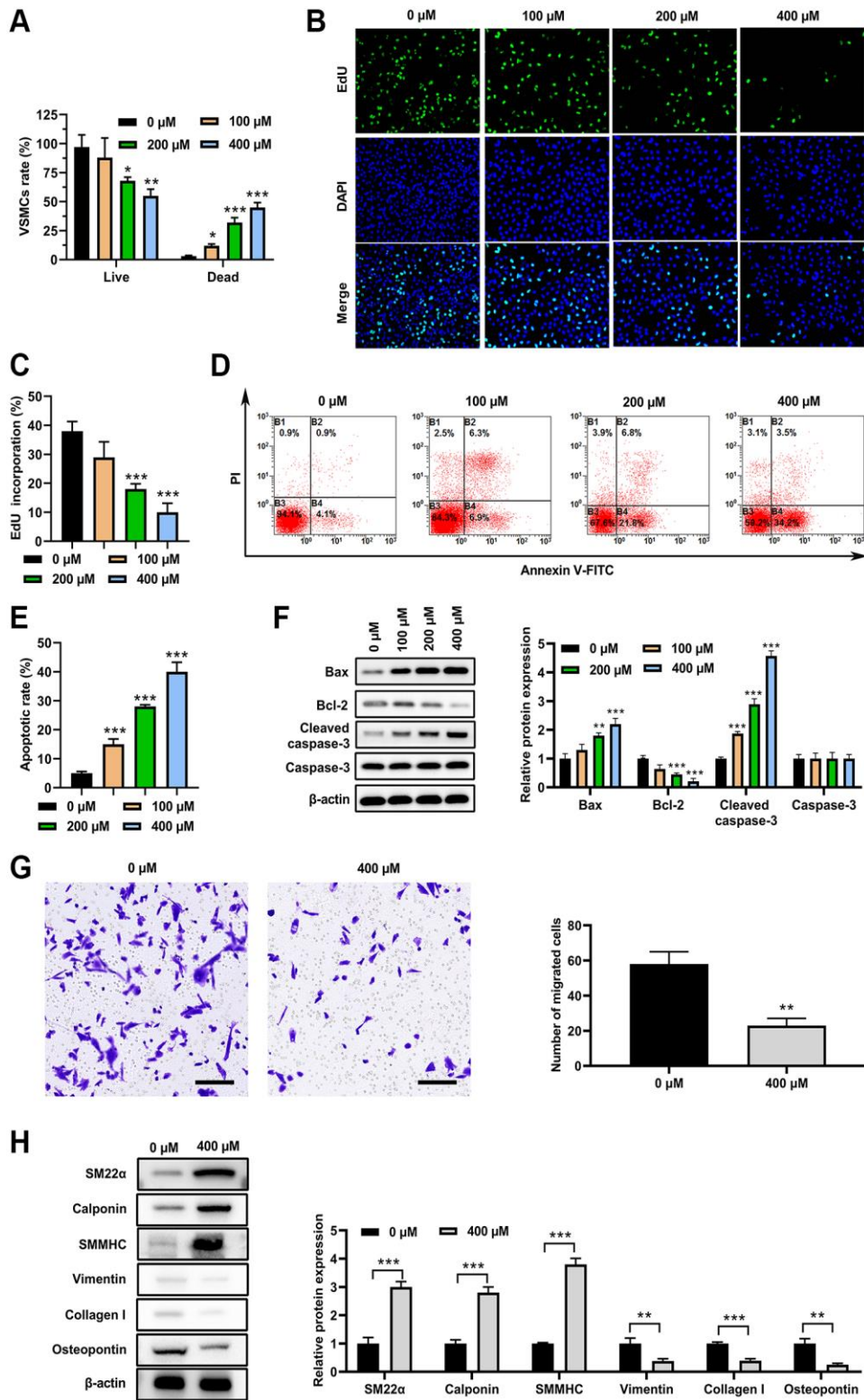


Figure 1. PA inhibited VSMC switch to synthetic phenotype. VSMC morphologies after PA treatments (0, 100, 200 or 400 μM) for 3d. (A) Live/dead cell assay of PA-treated VSMCs. (B and C). EdU assay to detect the proliferation on VSMCs treated with PA. (D and E). Flow cytometry to detect the apoptosis of PA-treated VSMCs. (F) Western blot determined the expression of apoptosis associated markers. (G) Transwell assay of PA-treated (200 μM) VSMCs. Scale bar = 100 μm . (H) Expression levels of SM22 α , calponin, SMMHC, vimentin, collagen I, and osteopontin in PA-treated (200 μM for 3 d) VSMCs. $n = 3$. * $P < 0.05$, ** $P < 0.01$.

miRNAs which are involved in alteration of VSMC phenotype switch were screened in PA-treated VSMCs. As shown in Figure 2A, 15 miRNAs were detected, and among these miRNAs, 3 miRNAs were increased and 1

miRNA were decreased in PA-treated VSMCs compared with that in untreated VSMCs. Following this, the top 3 increased miRNAs were overexpressed in VSMCs via using transfecting with their specific

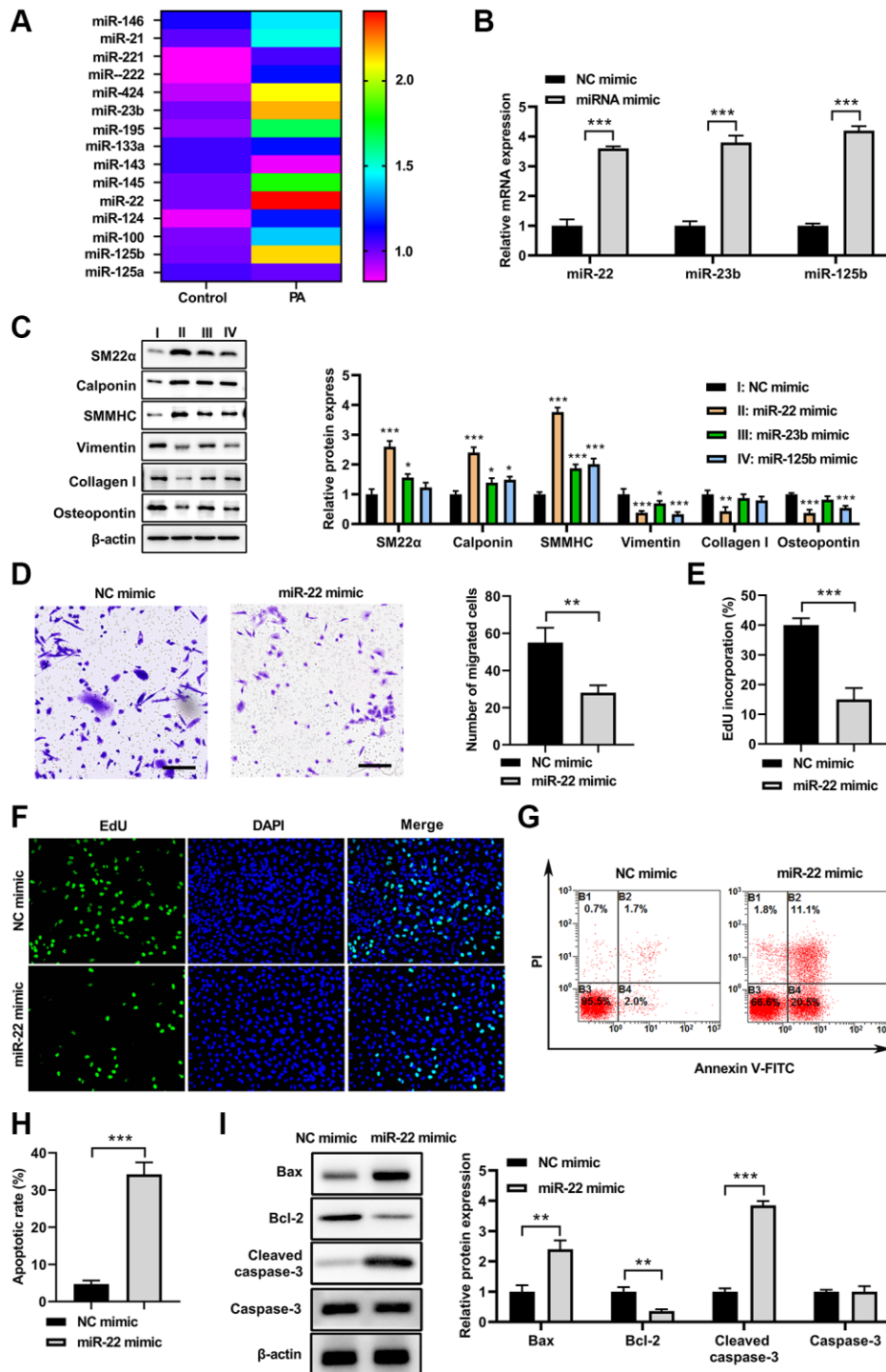


Figure 2. PA increased miR-22 expression in VSMCs. (A) MiRNAs levels in VSMCs treated with PA. (B) The mRNA levels of miR-22, miR-23b, and miR-125b in VSMCs after transfecting with their specific miRNA mimics. (C) The protein expression of SM22α, calponin, SMMHC, vimentin, collagen I, and osteopontin in VSMCs treated with miR-22, miR-23b or miR-125b mimics. (D) Migration ability of VSMCs transfecting with miR-22 mimics determined by transwell assay. Scale bar=100 μm. (E, F) The cell proliferation of VSMCs treated with miR-22 mimics detected by EdU assay. (G, H) Apoptosis of VSMCs treated with miR-22 mimics determined by flow cytometry. (I) The protein expression of bax, bcl-2, caspase-3, and cleaved-caspase-3 in VSMCs treated with miR-22 mimics. $n = 3$. * $P < 0.05$, ** $P < 0.01$.

miRNA mimics, respectively (Figure 2B). Following this, the expression of synthetic and contractile markers was detected in VSMCs. As shown in Figure 2C, miR-22, miR-23b, and miR-125b mimics all increased the mRNA levels for SM22 α , calponin, and SMMHC, and decreased mRNA levels of vimentin, collagen I, and OPN, suggesting that PA may inhibit the VSMC switch to synthetic phenotype via upregulation of these miRNAs. Specifically, miR-22 presented the most significant effect among these miRNAs. Thus, we had chosen miR-22 for the following investigation. Moreover, transwell assay suggested that increased expression of miR-22 mimics obviously inhibited the VSMCs migration (Figure 2D). Overexpression of miR-22 mimics also inhibited the proliferation of VSMCs (Figure 2E and 2F). In addition, flow cytometry suggested that overexpression of miR-22 mimic increased the apoptosis of VSMCs (Figure 2G and 2H). Correspondingly, the western blot analysis showed that miR-22 mimic increased the expression of Bax and cleaved-caspase-3, but decrease Bcl-2 expression (Figure 2I). These results suggested that PA may inhibit the VSMC switch to synthetic phenotype via upregulation of miR-22.

miR-22 inhibitor abolished the effects of PA on VSMC phenotype switch

To test whether miR-22 is involved in the PA's effects on VSMC phenotype switch, miR-22 inhibitor was used to inhibit the PA-upregulated miR-22. As shown in Figure 3A, miR-22 inhibitor decreased the miR-22 levels in VSMCs. As a result, PA treatment (200 μ M) significantly inhibited the cell viability but increased apoptosis in VSMCs, while overexpression of miR-22 inhibitor attenuated the impacts of PA on the proliferation and apoptosis of VSMCs (Figure 3B–3E). Correspondingly, the western blot analysis presented that overexpression of miR-22 inhibitor attenuated the effect of PA in increasing bax and cleaved-caspase-3 expression, and decreasing bcl-2 expression (Figure 3F). Transwell analysis showed that overexpression of PA treatment significantly decreased the migration of VSMCs, but miR-22 inhibitor obviously aborted this enhancement (Figure 3G). In addition, the western blot analyses showed that PA treatment obviously accumulated the expression of SM22 α , calponin, and SMMHC, but decreased the expression of vimentin, collagen I, and OPN; while overexpression of miR-22 inhibitor attenuated the effect of PA in VSMCs (Figure 3H). These results reinforced the notion that PA inhibits the VSMC switch to synthetic phenotype.

EVI1 was the target of miR-22

The potential target genes of miR-22 were predicted by miRDB, ENCOR1, and TargetScan. There were 50

candidates (Figure 4A), and 10 of them are associate with cell proliferation, migration, or apoptosis (Figure 4B). Among these candidates, overexpression of miR-22 reduced EVI1 mRNA levels significantly in VSMCs (Figure 4B). Western blot array showed the miR-22 mimic could significantly decrease the EVI1 expression, but miR-22 inhibitor largely enhanced the EVI1 expression (Figure 4C and 4D), indicating EVI1 acted as a candidate target of miR-22. This result was further confirmed by dual-luciferase reporter assay and presented that miR-22 reduced luciferase activity for EVI1 wild-type 3'UTR constructs but had no effect on the mutated binding site (Figure 4E and 4F). In addition, PA treatment abolished the EVI1 protein expression, while miR-22 inhibitor attenuated these downregulation, thereby upregulating EVI1 expression (Figure 4G). These results suggested that EVI1 is a target of miR-22.

PA treatment enhanced the effect of miR-22 on abolishing EVI1 mediated VSMC phenotype switch

To test whether EVI1 contributes to the effects of PA on VSMC phenotype switch, EVI1 and miR-22 were overexpressed in VSMCs followed by PA treatment. The qRT-PCR demonstrated that EVI1 overexpression did not change the levels of miR-22 in VSMCs, but PA treatment could enhance the upregulation of miR-22 (Figure 5A). Overexpression of miR-22 mimic significantly suppressed the EVI1 expression and PA treatment further enhanced this inhibition on the expression of EVI1 (Figure 5A). Moreover, PA treatment promoted cell proliferation as detected by EdU staining in VSMCs with EVI1 overexpression, while miR-22 mimic expression aborted this upregulation and PA treatment markedly enhanced this inhibitive effect mediated by miR-22 (Figure 5B). Flow cytometry analysis presented that overexpression of EVI1 had no obvious effect on the apoptosis of VSMCs, but miR-22 and PA treatment could enhance the apoptosis of EVI1 (Figure 5C). Similarly, EVI1 had no obviously effect on the expression of bax, bcl-2, caspase-3, and cleaved caspase-3, while miR-22 mimic and PA treatment could significantly promote the bax and cleaved-caspase-3 but decreased bcl-2 expression (Figure 5D). Transwell assays indicated that EVI1 significantly increased the migration of VSMCs, while miR-22 and PA treatment obviously attenuated this promotion to suppress the migration of VSMCs (Figure 5E and 5F). In addition, EVI1 also inhibited the contractile markers of SM22 α , calponin, and SMMHC and promoted the synthetic markers of vimentin, collagen I, and OPN, while miR-22 and PA treatment attenuated these changes (Figure 5G). These results reinforced the notion that PA inhibits the VSMC switch to synthetic phenotype through regulation of miR-22/EVI1 axis.

DISCUSSION

Mounting evidence has shown that disorder in fatty acid metabolism plays a casual role in the development of

atherosclerosis and other vascular diseases [9, 10]. However, how fatty acid regulates VSMC phenotype switch has not been studied. Here, we found that PA, the most common saturated fatty acid in circulation,

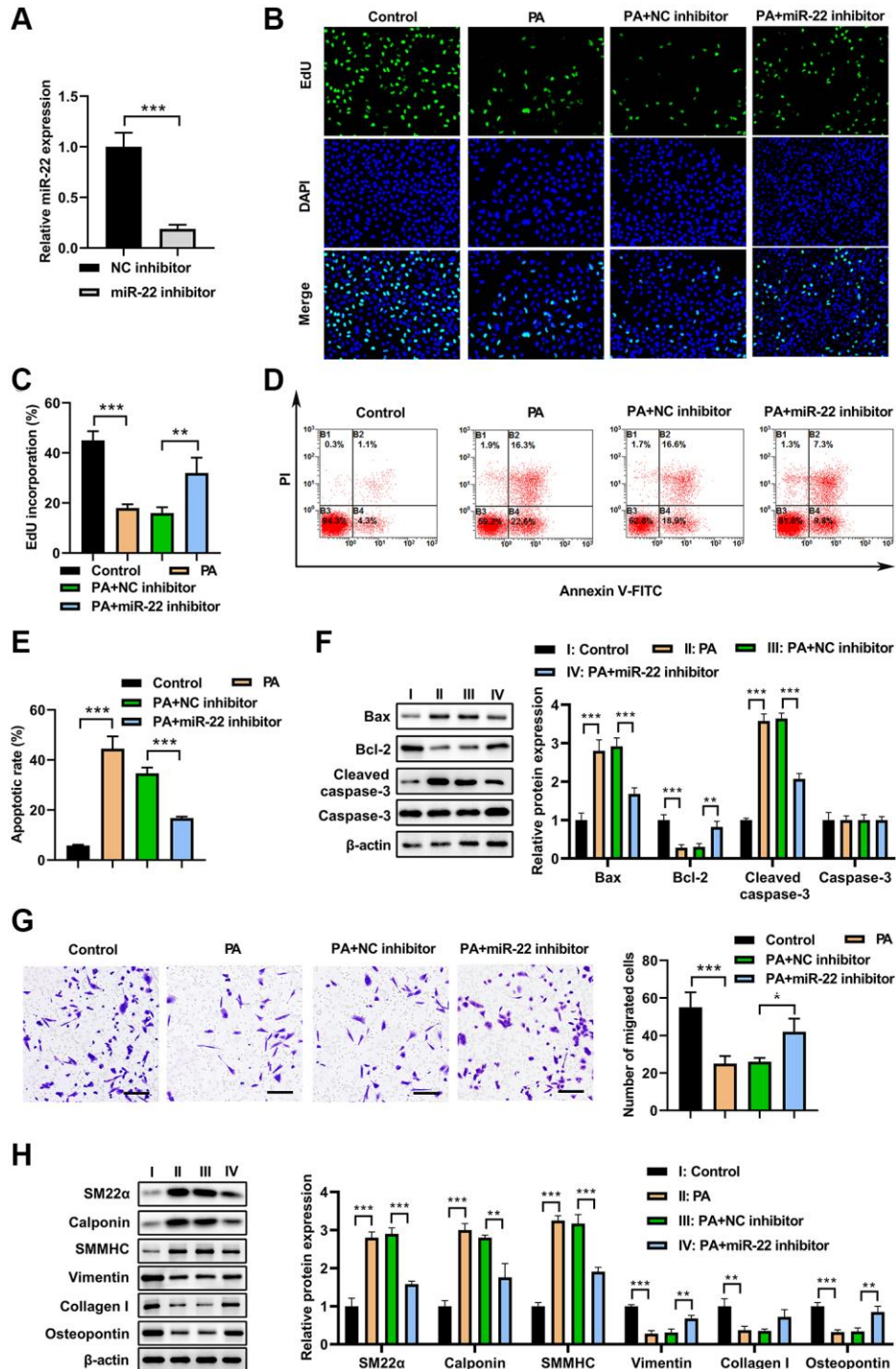


Figure 3. miR-22 inhibitor abolished the effects of PA on VSMC phenotype switch. (A) MiR-22 inhibitor decreased the miR-22 levels in VSMCs. (B, C) The proliferation of VSMCs transfected with miR-22 inhibitor or/and 200 μ M PA. (D, E) The apoptosis of VSMCs transfected with miR-22 inhibitor or/and 200 μ M PA. (F) The expression of apoptosis associated markers in VSMCs transfected with miR-22 inhibitor or/and 200 μ M PA. (G) The migration of VSMCs transfected with miR-22 inhibitor or/and 200 μ M PA determined by transwell assay. Scale bar=100 μ m. (H) Western blot analyses showing that expression of SM22 α , calponin, SMMHC, vimentin, collagen I, and osteopontin in PA-treated VSMCs transfected with miR-22 inhibitor. $n = 3$. * $P < 0.05$, ** $P < 0.01$.

inhibited VSMC switch to synthetic phenotype, as manifested by inhibiting VSMC proliferation, migration, and synthesis. Mechanistically, PA inhibits VSMC switch to synthetic phenotype through upregulation of miR-22 by targeting EVI1. These findings suggested that PA plays a role in the regulation

of VSMC phenotype, which may contribute to vascular health and diseases.

Several studies have shown that saturated fatty acids increase the risk of cardiovascular diseases [12, 28]. According to the previous study, the saturated fatty

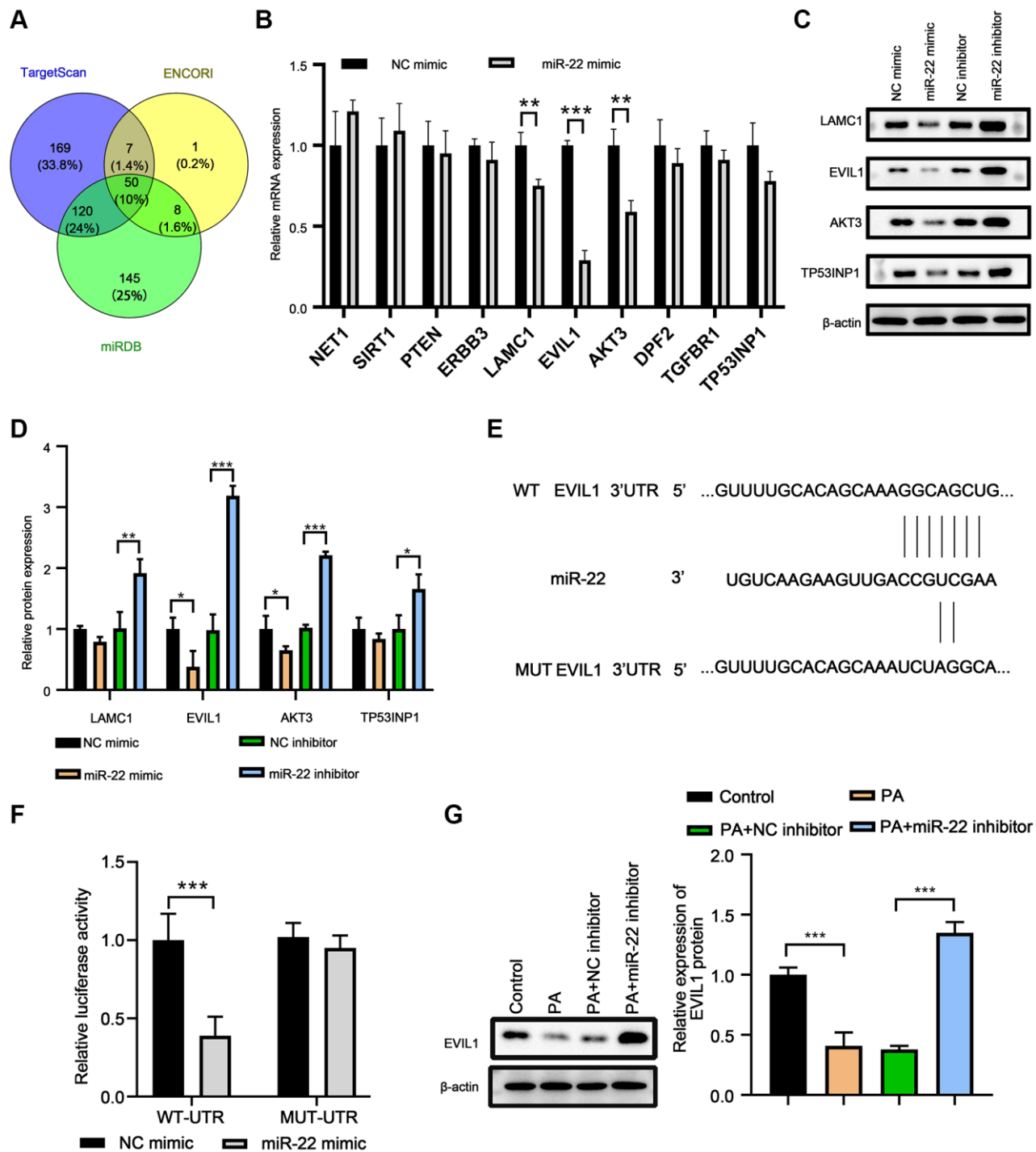


Figure 4. EVI1 was the target of miR-22. (A) Target genes of miR-22 were predicted by miRDB, TargetScan and ENCORI. (B) MRNA levels of target genes in VSMCs treated with miR-22 mimics. (C, D) Protein levels of SM22 α , calponin, SMMHC, vimentin, collagen I, and osteopontin in VSMCs detected by western blot. (E) The complementary sequence between 3'-UTR of EVI1 and miR-22. (F) Dual-luciferase reporter assay. (G) EVI1 protein level was detected by western blot in VSMCs treated with miR-22 inhibitor or PA. $n = 3$. * $P < 0.05$, ** $P < 0.01$.

acids were usually regarded as a singular fatty acid group and they might have the same effects during the metabolism [29, 30]. However, some investigations

focused on different biomarkers of risk of cardiovascular diseases found that not all SFAs exert the same effect, namely, studies do not seem to serve as

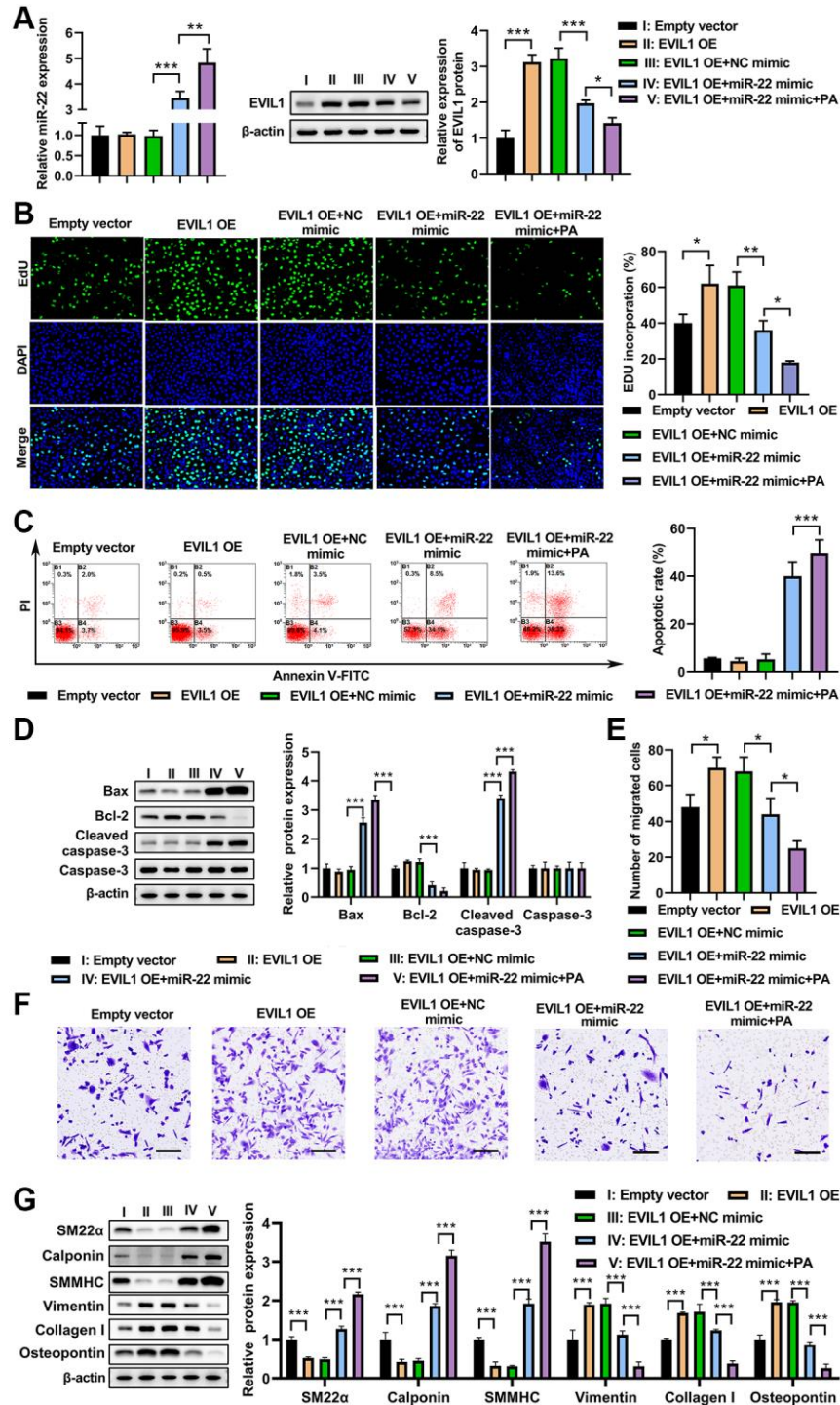


Figure 5. PA treatment enhanced miR-22 mimic impacts on aborted the inhibitive effect of EVI1 on VSMC phenotype switch. (A) Expression of miR-22 and EVI1 in VSMCs treated with EVI1 or/and miR-22 overexpression followed by PA treatment. (B) Cell proliferation was detected by EdU in VSMCs with EVI1/miR-22 overexpression followed by PA treatment. (C) Flow cytometry to detect the apoptosis of VSMCs with EVI1/miR-22 overexpression followed by PA treatment. (D) Western blot to detect the apoptosis associated markers in VSMCs. (E, F) Cell migration was detected by transwell assay in EVI1/miR-22-overexpressed VSMCs followed by PA treatment. Scale bar = 100 μ m. (G) Protein levels of SM22 α , calponin, SMMHC, vimentin, collagen I, and osteopontin in VSMC in VSMCs with EVI1/miR-22 overexpression followed by PA treatment detected by western blot. $n = 3$. * $P < 0.05$, ** $P < 0.01$.

a single role of PA in the development of cardiovascular diseases [31]. PA slightly elevated the LDL- and HDL-cholesterol, which is a significant predictor for cardiovascular disease [32, 33]. Although the role of PA in cardiovascular diseases needs to be further examined, these advances suggest that PA's effects in cardio-vascular health and disease cannot be easily identified as detrimental or beneficial. Here, we found that PA inhibited VSMC switch to synthetic phenotype, as manifested by inhibiting VSMC proliferation, migration, and synthesis, suggesting that PA may exert beneficial effects on vascular health and diseases, which should be identified by further studies.

Recent studies support a critical role of miRNAs in regulating VSMC differentiation and phenotype switch, and miR-22 is one of the miRNAs which inhibits VSMC switch to synthetic phenotype [16, 17]. miR-22 is previously demonstrated as a tumor suppressor, but later has been concerned as a prohypertrophic miRNA [34, 35]. A recent study documented that miR-22 playing key role in the regulation role in VSMC biological activity [36]. In addition, it has also been reported that miR-22 involved in VSMC phenotypic modulation, which induces VSMC contractile gene expression, but inhibits VSMC proliferation and migration [17]. These findings indicated that miR-22 serves a key role in regulation of cardiovascular function. Here, we show that PA increased miR-22 expression in VSMCs, and inhibition of miR-22 abolished the PA's effects on modulation of VSMC phenotype. It has been reported that transforming growth factor- β 1 (TGF- β 1) transcriptionally modulates miR-22 expression in VSMCs via a P53-dependent mechanism [17]. Whether PA regulates miR-22 expression through TGF- β 1 needed further investigation. Indeed, there is evidence that PA treatment increases TGF- β 1 in other cells [37]. These findings suggested that PA modulate VSMC phenotype via upregulating miR-22, which serves a crucial role vascular function regulation.

Previous studies demonstrated that EVI1 functions as a transcriptional regulator to modulate several biological processes, including hematopoiesis, apoptosis, development, differentiation and proliferation [38, 39]. Here, we have found that EVI1 serves as a target gene of miR-22 to modulate VSMC phenotype switch. Further analysis showed that EVI1 transcriptionally inhibits VSMC-specific genes to modulate the VSMC phenotype switch, including SM α A, SM22 α , SRF, and Myocd [17]. In addition, inhibiting EVI1 abolished the effects of miR-22 and PA in modulation of VSMC phenotype. These findings suggested that miR-22/EVI1

signaling axis plays a key role in VSMC phenotypic switch and correcting the dysregulation of miR-22/EVI1 or PA could be a potential treatment to vascular diseases.

CONCLUSION

Taken together, we found that PA inhibits VSMC switch to synthetic phenotype through upregulation of miR-22 expression. In addition, miR22 inhibits VSMC switch to synthetic phenotype by targeting EVI1. These findings suggested that PA plays a role in regulation of VSMC phenotype, which may contribute to maintenance of vascular health and prevention of vascular diseases.

Abbreviations

VSMC: Vascular smooth muscle cell; PA: palmitic acid; EVI1: ecotropic virus integration site 1 protein homolog.

AUTHOR CONTRIBUTIONS

Yanchao Hu and Congxia Wang conceived and designed these experiments. Yajie Fan and Chunyan Zhang performed these experiments. Yajie Fan and Chunyan Zhang analyzed and interpreted the data. Yanchao Hu and Congxia Wang wrote the manuscript. All authors read and approved the final manuscript.

CONFLICTS OF INTEREST

All authors have completed the ICMJE uniform disclosure form. All the authors declare that they have no competing interests.

ETHICAL STATEMENT

All animal procedures in this study were conducted in accordance with the National Institutes of Health Guidelines on the Use of Laboratory Animals. The study protocol was approved by the Ethics Committee of Xi'an Jiaotong University Second Affiliated Hospital. Animal care and study were approved by the Institutional Animal Care and Use Committee of Xi'an Jiaotong University Second Affiliated Hospital.

FUNDING

The Key R&D Project of Shaanxi Province in 2021: the role of urotensin II and transforming growth factor β 1 in ventricular remodeling of chronic heart failure (No. 2021SF-321).

Editorial note

&This corresponding author has a verified history of publications using a personal email address for correspondence.

REFERENCES

1. Basatemur GL, Jørgensen HF, Clarke MCH, Bennett MR, Mallat Z. Vascular smooth muscle cells in atherosclerosis. *Nat Rev Cardiol*. 2019; 16:727–44. <https://doi.org/10.1038/s41569-019-0227-9> PMID:[31243391](https://pubmed.ncbi.nlm.nih.gov/31243391/)
2. Bennett MR, Sinha S, Owens GK. Vascular Smooth Muscle Cells in Atherosclerosis. *Circ Res*. 2016; 118:692–702. <https://doi.org/10.1161/CIRCRESAHA.115.306361> PMID:[26892967](https://pubmed.ncbi.nlm.nih.gov/26892967/)
3. Lacolley P, Regnault V, Avolio AP. Smooth muscle cell and arterial aging: basic and clinical aspects. *Cardiovasc Res*. 2018; 114:513–28. <https://doi.org/10.1093/cvr/cvy009> PMID:[29514201](https://pubmed.ncbi.nlm.nih.gov/29514201/)
4. Morrow D, Guha S, Sweeney C, Birney Y, Walshe T, O'Brien C, Walls D, Redmond EM, Cahill PA. Notch and vascular smooth muscle cell phenotype. *Circ Res*. 2008; 103:1370–82. <https://doi.org/10.1161/CIRCRESAHA.108.187534> PMID:[19059839](https://pubmed.ncbi.nlm.nih.gov/19059839/)
5. Grootaert MOJ, Moulis M, Roth L, Martinet W, Vindis C, Bennett MR, De Meyer GRY. Vascular smooth muscle cell death, autophagy and senescence in atherosclerosis. *Cardiovasc Res*. 2018; 114:622–34. <https://doi.org/10.1093/cvr/cvy007> PMID:[29360955](https://pubmed.ncbi.nlm.nih.gov/29360955/)
6. Chistiakov DA, Orekhov AN, Bobryshev YV. Vascular smooth muscle cell in atherosclerosis. *Acta Physiol (Oxf)*. 2015; 214:33–50. <https://doi.org/10.1111/apha.12466> PMID:[25677529](https://pubmed.ncbi.nlm.nih.gov/25677529/)
7. Salabei JK, Hill BG. Autophagic regulation of smooth muscle cell biology. *Redox Biol*. 2015; 4:97–103. <https://doi.org/10.1016/j.redox.2014.12.007> PMID:[25544597](https://pubmed.ncbi.nlm.nih.gov/25544597/)
8. Yang L, Gao L, Nickel T, Yang J, Zhou J, Gilbertsen A, Geng Z, Johnson C, Young B, Henke C, Gourley GR, Zhang J. Lactate Promotes Synthetic Phenotype in Vascular Smooth Muscle Cells. *Circ Res*. 2017; 121:1251–62. <https://doi.org/10.1161/CIRCRESAHA.117.311819> PMID:[29021296](https://pubmed.ncbi.nlm.nih.gov/29021296/)
9. Matsushita T, Ikeda S, Miyahara Y, Yakabe K, Yamaguchi K, Furukawa K, Iwasaki T, Shikuwa M, Fukui J, Kohno S. Use of [123I]-BMIPP myocardial scintigraphy for the clinical evaluation of a fatty-acid metabolism disorder of the right ventricle in chronic respiratory and pulmonary vascular disease. *J Int Med Res*. 2000; 28:111–23. <https://doi.org/10.1177/147323000002800302> PMID:[10983861](https://pubmed.ncbi.nlm.nih.gov/10983861/)
10. Semenkovich CF. Fatty acid metabolism and vascular disease. *Trends Cardiovasc Med*. 2004; 14:72–6. <https://doi.org/10.1016/j.tcm.2003.12.004> PMID:[15030793](https://pubmed.ncbi.nlm.nih.gov/15030793/)
11. Berry SE. Triacylglycerol structure and interesterification of palmitic and stearic acid-rich fats: an overview and implications for cardiovascular disease. *Nutr Res Rev*. 2009; 22:3–17. <https://doi.org/10.1017/S0954422409369267> PMID:[19442321](https://pubmed.ncbi.nlm.nih.gov/19442321/)
12. Fattore E, Fanelli R. Palm oil and palmitic acid: a review on cardiovascular effects and carcinogenicity. *Int J Food Sci Nutr*. 2013; 64:648–59. <https://doi.org/10.3109/09637486.2013.768213> PMID:[23406428](https://pubmed.ncbi.nlm.nih.gov/23406428/)
13. Micha R, Mozaffarian D. Saturated fat and cardiometabolic risk factors, coronary heart disease, stroke, and diabetes: a fresh look at the evidence. *Lipids*. 2010; 45:893–905. <https://doi.org/10.1007/s11745-010-3393-4> PMID:[20354806](https://pubmed.ncbi.nlm.nih.gov/20354806/)
14. Alexander MR, Owens GK. Epigenetic control of smooth muscle cell differentiation and phenotypic switching in vascular development and disease. *Annu Rev Physiol*. 2012; 74:13–40. <https://doi.org/10.1146/annurev-physiol-012110-142315> PMID:[22017177](https://pubmed.ncbi.nlm.nih.gov/22017177/)
15. Gomez D, Owens GK. Smooth muscle cell phenotypic switching in atherosclerosis. *Cardiovasc Res*. 2012; 95:156–64. <https://doi.org/10.1093/cvr/cvs115> PMID:[22406749](https://pubmed.ncbi.nlm.nih.gov/22406749/)
16. Tang Y, Yu S, Liu Y, Zhang J, Han L, Xu Z. MicroRNA-124 controls human vascular smooth muscle cell phenotypic switch via Sp1. *Am J Physiol Heart Circ Physiol*. 2017; 313:H641–9. <https://doi.org/10.1152/ajpheart.00660.2016> PMID:[28667053](https://pubmed.ncbi.nlm.nih.gov/28667053/)
17. Yang F, Chen Q, He S, Yang M, Maguire EM, An W, Afzal TA, Luong LA, Zhang L, Xiao Q. miR-22 Is a Novel Mediator of Vascular Smooth Muscle Cell Phenotypic Modulation and Neointima Formation. *Circulation*.

- 2018; 137:1824–41.
<https://doi.org/10.1161/CIRCULATIONAHA.117.027799>
PMID:[29246895](https://pubmed.ncbi.nlm.nih.gov/29246895/)
18. Wang M, Li W, Chang GQ, Ye CS, Ou JS, Li XX, Liu Y, Cheang TY, Huang XL, Wang SM. MicroRNA-21 regulates vascular smooth muscle cell function via targeting tropomyosin 1 in arteriosclerosis obliterans of lower extremities. *Arterioscler Thromb Vasc Biol.* 2011; 31:2044–53.
<https://doi.org/10.1161/ATVBAHA.111.229559>
PMID:[21817107](https://pubmed.ncbi.nlm.nih.gov/21817107/)
 19. Iaconetti C, De Rosa S, Polimeni A, Sorrentino S, Gareri C, Carino A, Sabatino J, Colangelo M, Curcio A, Indolfi C. Down-regulation of miR-23b induces phenotypic switching of vascular smooth muscle cells in vitro and in vivo. *Cardiovasc Res.* 2015; 107:522–33.
<https://doi.org/10.1093/cvr/cvv141>
PMID:[25994172](https://pubmed.ncbi.nlm.nih.gov/25994172/)
 20. Grundmann S, Hans FP, Kinniry S, Heinke J, Helbing T, Bluhm F, Sluijter JP, Hoefer I, Pasterkamp G, Bode C, Moser M. MicroRNA-100 regulates neovascularization by suppression of mammalian target of rapamycin in endothelial and vascular smooth muscle cells. *Circulation.* 2011; 123:999–1009.
<https://doi.org/10.1161/CIRCULATIONAHA.110.000323>
PMID:[21339483](https://pubmed.ncbi.nlm.nih.gov/21339483/)
 21. Torella D, Iaconetti C, Catalucci D, Ellison GM, Leone A, Waring CD, Bochicchio A, Vicinanza C, Aquila I, Curcio A, Condorelli G, Indolfi C. MicroRNA-133 controls vascular smooth muscle cell phenotypic switch in vitro and vascular remodeling in vivo. *Circ Res.* 2011; 109:880–93.
<https://doi.org/10.1161/CIRCRESAHA.111.240150>
PMID:[21852550](https://pubmed.ncbi.nlm.nih.gov/21852550/)
 22. Yue Y, Zhang Z, Zhang L, Chen S, Guo Y, Hong Y. miR-143 and miR-145 promote hypoxia-induced proliferation and migration of pulmonary arterial smooth muscle cells through regulating ABCA1 expression. *Cardiovasc Pathol.* 2018; 37:15–25.
<https://doi.org/10.1016/j.carpath.2018.08.003>
PMID:[30195228](https://pubmed.ncbi.nlm.nih.gov/30195228/)
 23. Luo Y, Xiong W, Dong S, Liu F, Liu H, Li J. MicroRNA-146a promotes the proliferation of rat vascular smooth muscle cells by downregulating p53 signaling. *Mol Med Rep.* 2017; 16:6940–5.
<https://doi.org/10.3892/mmr.2017.7477>
PMID:[28901447](https://pubmed.ncbi.nlm.nih.gov/28901447/)
 24. Ji Z, Chi J, Sun H, Ru A, Ni T, Zhang J, Jiang F, Lv H, Peng F, Guo H, Chen Y. Linc-ROR targets FGF2 to regulate HASMC proliferation and migration via sponging miR-195-5p. *Gene.* 2020; 725:144143.
<https://doi.org/10.1016/j.gene.2019.144143>
PMID:[31629816](https://pubmed.ncbi.nlm.nih.gov/31629816/)
 25. Liu X, Cheng Y, Zhang S, Lin Y, Yang J, Zhang C. A necessary role of miR-221 and miR-222 in vascular smooth muscle cell proliferation and neointimal hyperplasia. *Circ Res.* 2009; 104:476–87.
<https://doi.org/10.1161/CIRCRESAHA.108.185363>
PMID:[19150885](https://pubmed.ncbi.nlm.nih.gov/19150885/)
 26. Merlet E, Atassi F, Motiani RK, Mougenot N, Jacquet A, Nadaud S, Capiod T, Trebak M, Lompré AM, Marchand A. miR-424/322 regulates vascular smooth muscle cell phenotype and neointimal formation in the rat. *Cardiovasc Res.* 2013; 98:458–68.
<https://doi.org/10.1093/cvr/cvt045>
PMID:[23447642](https://pubmed.ncbi.nlm.nih.gov/23447642/)
 27. Tang R, Mei X, Wang YC, Cui XB, Zhang G, Li W, Chen SY. LncRNA GAS5 regulates vascular smooth muscle cell cycle arrest and apoptosis via p53 pathway. *Biochim Biophys Acta Mol Basis Dis.* 2019; 1865:2516–25.
<https://doi.org/10.1016/j.bbadis.2019.05.022>
PMID:[31167125](https://pubmed.ncbi.nlm.nih.gov/31167125/)
 28. Kritchevsky D. Overview: Dietary fat and atherosclerosis. *Asia Pac J Clin Nutr.* 2000; 9:141–5.
<https://doi.org/10.1046/j.1440-6047.2000.00140.x>
PMID:[24394402](https://pubmed.ncbi.nlm.nih.gov/24394402/)
 29. Cater NB, Heller HJ, Denke MA. Comparison of the effects of medium-chain triacylglycerols, palm oil, and high oleic acid sunflower oil on plasma triacylglycerol fatty acids and lipid and lipoprotein concentrations in humans. *Am J Clin Nutr.* 1997; 65:41–5.
<https://doi.org/10.1093/ajcn/65.1.41>
PMID:[8988911](https://pubmed.ncbi.nlm.nih.gov/8988911/)
 30. Karupaiah T, Tan CH, Chinna K, Sundram K. The chain length of dietary saturated fatty acids affects human postprandial lipemia. *J Am Coll Nutr.* 2011; 30:511–21.
<https://doi.org/10.1080/07315724.2011.10719997>
PMID:[22331686](https://pubmed.ncbi.nlm.nih.gov/22331686/)
 31. Karupaiah T, Sundram K. Effects of stereospecific positioning of fatty acids in triacylglycerol structures in native and randomized fats: a review of their nutritional implications. *Nutr Metab (Lond).* 2007; 4:16.
<https://doi.org/10.1186/1743-7075-4-16>
PMID:[17625019](https://pubmed.ncbi.nlm.nih.gov/17625019/)
 32. Clandinin MT, Cook SL, Konard SD, French MA. The effect of palmitic acid on lipoprotein cholesterol levels. *Int J Food Sci Nutr.* 2000 (Suppl); 51:S61–71.
PMID:[11271858](https://pubmed.ncbi.nlm.nih.gov/11271858/)
 33. Clandinin MT, Cook SL, Konrad SD, Goh YK, French MA. The effect of palmitic acid on lipoprotein cholesterol levels and endogenous cholesterol synthesis in hyperlipidemic subjects. *Lipids.* 1999

- (Suppl); 34:S121–4.
<https://doi.org/10.1007/BF02562257>
PMID:[10419117](https://pubmed.ncbi.nlm.nih.gov/10419117/)
34. Gurha P, Abreu-Goodger C, Wang T, Ramirez MO, Drummond AL, van Dongen S, Chen Y, Bartonicek N, Enright AJ, Lee B, Kelm RJ Jr, Reddy AK, Taffet GE, et al. Targeted deletion of microRNA-22 promotes stress-induced cardiac dilation and contractile dysfunction. *Circulation*. 2012; 125:2751–61.
<https://doi.org/10.1161/CIRCULATIONAHA.111.044354>
PMID:[22570371](https://pubmed.ncbi.nlm.nih.gov/22570371/)
35. Huang ZP, Chen J, Seok HY, Zhang Z, Kataoka M, Hu X, Wang DZ. MicroRNA-22 regulates cardiac hypertrophy and remodeling in response to stress. *Circ Res*. 2013; 112:1234–43.
<https://doi.org/10.1161/CIRCRESAHA.112.300682>
PMID:[23524588](https://pubmed.ncbi.nlm.nih.gov/23524588/)
36. Xiao Q, Zeng L, Zhang Z, Margariti A, Ali ZA, Channon KM, Xu Q, Hu Y. Sca-1+ progenitors derived from embryonic stem cells differentiate into endothelial cells capable of vascular repair after arterial injury. *Arterioscler Thromb Vasc Biol*. 2006; 26:2244–51.
<https://doi.org/10.1161/01.ATV.0000240251.50215.50>
PMID:[16902164](https://pubmed.ncbi.nlm.nih.gov/16902164/)
37. Duan NN, Liu XJ, Wu J. Palmitic acid elicits hepatic stellate cell activation through inflammasomes and hedgehog signaling. *Life Sci*. 2017; 176:42–53.
<https://doi.org/10.1016/j.lfs.2017.03.012>
PMID:[28322865](https://pubmed.ncbi.nlm.nih.gov/28322865/)
38. Wieser R. The oncogene and developmental regulator EVI1: expression, biochemical properties, and biological functions. *Gene*. 2007; 396:346–57.
<https://doi.org/10.1016/j.gene.2007.04.012>
PMID:[17507183](https://pubmed.ncbi.nlm.nih.gov/17507183/)
39. Yuan X, Wang X, Bi K, Jiang G. The role of EVI-1 in normal hematopoiesis and myeloid malignancies (Review). *Int J Oncol*. 2015; 47:2028–36.
<https://doi.org/10.3892/ijo.2015.3207>
PMID:[26496831](https://pubmed.ncbi.nlm.nih.gov/26496831/)

SUPPLEMENTARY MATERIALS

Supplementary Table

Supplementary Table 1. The primer sequences.

Gene	Primer (5'–3')
MYH11	F: AGGCGAACCTAGACAAGAATAAG R: CTGGATGTTGAGAGTGGAGATG
SM22 α	F: TTCTGCCTCAACATGGCCAAC3 R: CACCTTCACTGG CTTGGATC
Calponin	F: ATGTCCTCTGCTCACTTCAAC R: CACGTTACCTTGTTCCTTTC
SMMHC	F: AGGCGAACCTAGACAAGAATAAG R: CTGGATGTTGAGAGTGGAGATG
Collagen I	F: TGACGAGACCAAGAACTGCC R: GCACCATCATTTCACGAGC
Vimentin	F: TCGTTTCGAGGTTTTTCGCGTTAGAGAC R: GACTAAAACCTCGACCGACTCGCGA
Osteopontin	F: CAGCCTTCTCAGCCAAACG R: CAAATCACTGCAATTCTCATGGTAGT
MiR-22	F: AAGCTGCCAGTTGAAGAAGTGT R: Universal PCR Reverse Primer (cat. no. B532451; Sangon Biotech Co., Ltd.)
miR-23b	F: ATCACATTGCCAGGGATTACCAC R: Universal PCR Reverse Primer (cat. no. B532451; Sangon Biotech Co., Ltd.)
miR-125b	F: TCCCTGAGACCCTAACTTGTGA R: Universal PCR Reverse Primer (cat. no. B532451; Sangon Biotech Co., Ltd.)
NET1	F: AAATCCCCGGATGACGGC R: TGCACTGCTCCTTCTCTTGG
SIRT1	F: GCTCGCCTTGCGGTGGACTT R: GACGGCTGGAAGTGTCCGGG
PTEN	F: AGCCTCTTGATGTGTGCATT R: CCATTGGTAGCCAAACGGAAC
ERBB3	F: CATCGTGAGGGACCGAGATG R: TGTTGCTCGAGTCCACAGTC
LAMC1	F: GAGGCAAGATATCGCCGTGA R: GTATCTCGCCTGTCCACTCG
AKT3	F: GGTGCAGAGTCCCCTAGAGA R: TTGGCGACAGCAGGATCATT
DPF2	F: TGCCTGTGACATTTGTGGAA R: TAGCCACGATCGCAGTCATC
TGFBR1	F: TCCAACACTGGTTTACCATTGC R: ACAGCAACTTCTTCTCCCCG
TP53INP1	F: CGTCTGGGTACCTGAACGAG R: ACTTCTGTGCCCGTGAGTCT
EVI1	F: GCAGACATTGCGCCTGGGGAA

GAPDH

R: CTCACAGCGGTGCTGCCGTT

F: AACTTTGGCATTGTGGAAGG

R: ATTGGGGGTAGGAACA

U6

F: TGAGAACTGAATCCATGGGTT

R: ACGCTCACGAATTTGCGT
